



Adenosine A2A Receptor: A New Neuroprotective Target in Light-Induced Retinal Degeneration

Manuel Soliño^{1†}, Ignacio M. Larrayoz^{2†}, Ester María López^{1§}, Manuel Rey-Funes¹, Mariana Bareiro¹, Cesar Fabián Loidl¹, Elena Girardi¹, Alfredo Martínez^{3‡} and Juan José López-Costa^{1*‡}

¹Instituto de Biología Celular y Neurociencia "Prof. E. De Robertis" (IBCN), UBA-CONICET, Facultad de Medicina, Universidad de Buenos Aires, Ciudad Autónoma de Buenos Aires, Argentina, ²Biomarkers and Molecular Signaling Group, Center for Biomedical Research of La Rioja (CIBIR), Logroño, Spain, ³Angiogenesis Study Group, Center for Biomedical Research of La Rioja (CIBIR), Logroño, Spain

OPEN ACCESS

Edited by:

Georgina Rodríguez de Lores Arnaiz, Consejo Nacional de Investigaciones Científicas y Técnicas (CONICET), Argentina

Reviewed by:

Rodrigo A. Cunha, University of Coimbra, Portugal
Ana Raquel Santiago, University of Coimbra, Portugal

*Correspondence:

Juan José López-Costa
jjlopez@fmed.uba.ar

[†]These authors share first authorship

[‡]These authors share last authorship

[§]Died in February 2021

Specialty section:

This article was submitted to Neuropharmacology, a section of the journal Frontiers in Pharmacology

Received: 20 December 2021

Accepted: 14 February 2022

Published: 21 March 2022

Citation:

Soliño M, Larrayoz IM, López EM, Rey-Funes M, Bareiro M, Loidl CF, Girardi E, Martínez A and López-Costa JJ (2022) Adenosine A2A Receptor: A New Neuroprotective Target in Light-Induced Retinal Degeneration. *Front. Pharmacol.* 13:840134. doi: 10.3389/fphar.2022.840134

Continuous illumination induces the degeneration of photoreceptors. This animal model of light-induced retinal degeneration resembles many characteristics of human degenerative diseases of the outer retina, such as age-related macular degeneration. This work aimed to evaluate the potential neuroprotective effect of the modulation of adenosine A2A receptor in the model of light-induced retinal degeneration. Sprague-Dawley rats were intravitreally injected in the right eye with either CGS 21680, an adenosine A2A receptor agonist, or SCH 58261, an adenosine A2A receptor antagonist. Contralateral eyes were injected with respective vehicles as control. Then, rats were subjected to continuous illumination (12,000 lux) for 24 h. Retinas were processed by glial fibrillary acidic protein (GFAP) immunohistochemistry, terminal deoxynucleotidyl transferase dUTP nick end labeling (TUNEL) technique, Western blotting (WB), and quantitative reverse transcription-polymerase chain reaction (qRT-PCR). Another group of rats was subjected to functional studies by electroretinography. Animals treated with CGS21680 showed a significant increase of apoptotic nuclei in the outer nuclear layer and a significant increase of GFAP immunoreactive area of the retinas but did not alter WB nor electroretinography results. qRT-PCR showed that CGS 21680 significantly increased the expression of interleukin-1 β . On the opposite, SCH 58261 significantly decreased apoptotic nuclei in the outer nuclear layer and GFAP immunoreactive area of the retinas. It also significantly decreased GFAP and activated caspase-3 levels as measured by WB and preserved retinal function, as treated eyes showed significantly greater amplitudes of a- and b-waves and oscillatory potentials. qRT-PCR revealed that SCH 58261 significantly decreased the expression of tumor necrosis factor- α . These results show that the blockade of the A2A receptor before the start of the pathogenic process is neuroprotective, as it prevents light-induced retinal damage. The use of A2A receptor antagonists deserves to be evaluated in retinal degenerative diseases.

Keywords: Adenosine, retina, degeneration, A2A receptor, CGS 21680, SCH58261

INTRODUCTION

In recent years, the modulation of adenosine receptors has become a possible neuroprotective strategy to treat a wide range of insults and degenerative diseases of the central nervous system (CNS) (Stone et al., 2009). It has been reported that A1 receptor agonists are neuroprotective in animal models of inflammatory, hypoxic, epileptic, and degenerative diseases of the CNS (Boeck et al., 2005; Rosim et al., 2011; Gori and Girardi, 2013), whereas the use of A2A receptor agonists and/or antagonists has been useful against the neurotoxicity of 6-hydroxydopamine (Nobre et al., 2010), spinal cord injury (Paterniti et al., 2011), convulsions induced by pilocarpine (Rosim et al., 2011), memory dysfunction (Kaster et al., 2015), and degenerative diseases such as Alzheimer disease (Canas et al., 2009) and Parkinson's disease (Gyoneva et al., 2014; Jenner, 2014). A broader review of the neuroprotective role of A2A receptor modulation may be found in Cunha (2016).

The release of adenosine is an important component of the response to ischemic/hypoxic insults of the retina (Roth et al., 1997; Li et al., 1999), probably through the production of hyperemia that protects neurons from glutamate toxicity (Ostwald et al., 1997). The neuroprotective role of adenosine after ischemic retinal injury could be mediated by A1 (A1R) and/or A2 receptors (Housley et al., 2009).

Adenosine A1 and A2A receptors (A2AR) crosstalk with interleukin (IL)-6 and regulate the production of brain-derived neurotrophic factors (Perigolo-Vicente et al., 2014). The A2AR has been described as a transactivator of many other signaling families, including cannabinoids and neurotrophins (Tebano et al., 2010). The effect of adenosine receptors on other neurotrophins as glial cell line-derived neurotrophic factor and vascular endothelial growth factor seems to be responsible for the neuroprotective role of adenosine (Leibovich et al., 2002; Gomes et al., 2009). In the CNS and in the retina, it has been proposed that A2AR also plays a role in the microglial response to neuronal degenerative diseases (Santiago et al., 2014). The neuroprotective role of adenosine has been reviewed in different models of retinal degeneration, including ischemic retinopathy and diabetes (Dos Santos Rodrigues et al., 2015). Using a model of light-induced retinal degeneration (LIRD), which resembles many of the characteristics of age-related macular degeneration and retinitis pigmentosa (RP), we demonstrated that cyclopentyladenosine, an A1R agonist, protects the photoreceptors from light-induced damage, whereas dipropylcyclopentylxanthine, an A1R antagonist, has the opposite action (Soliño et al., 2018). Besides, the neuroprotective role of A2AR antagonists, such as KW6002 and SCH58261, has been demonstrated against the retinal damage induced by ischemia-reperfusion (Madeira et al., 2016a; Boia et al., 2017). Therefore, the present study aimed to investigate if the modulation of A2AR before the exposure to continuous illumination (CI) is able to prevent retinal damage in the model of LIRD as well.

MATERIALS AND METHODS

Animals

Male Sprague-Dawley albino rats ($n = 46$, body weight 200 g, age 60 days) were used.

Intravitreal Injections Protocol

Intravitreal injections were performed as previously described (Soliño et al., 2018). Briefly, general anesthesia was performed with ketamine (40 mg/kg; Ketamina 50, Holliday-Scott SA, Argentina) and xylazine (5 mg/kg; Kensol, König SA, Argentina), and in addition, local anesthesia was performed with 2% lidocaine (Lidocaine, Richmond SA, Argentina). Intravitreal injections (5 μ l) were performed using a Hamilton syringe (Reno, NV, United States) and a 30-gauge needle. The right eyes received either CGS21680 (Abcam plc, Cambridge, United Kingdom, ab120453), an A2AR agonist, or SCH58261 (Sigma-Aldrich Inc., St. Louis, MO, United States, CAS no. 160098-96-4), an A2AR antagonist. Meanwhile, the left eyes, which were the controls (CTL), received the vehicle. As the volume of vitreous of the rat eye is $13.36 \pm 0.64 \mu$ l (Dureau et al., 2001), the final vitreal concentrations were 0.9 mM for CGS 21680 and 0.066 mM for SCH 58261 in agreement with previous reports (Ongini, 1998; Font et al., 2008).

Light-Induced Retinal Degeneration Procedure

One hour after intravitreal injections, rats were continuously illuminated for 24 h at 12,000 lux as previously described (Soliño et al., 2018). Groups of 3–5 rats were simultaneously placed in an open white acrylic box of 60 cm \times 60 cm \times 60 cm with 12 halogen lamps (12 V, 50 W each) located on top. Lighting level and temperature (21°C) were monitored. Then, the retinas were obtained around 2 p.m. and processed for glial fibrillary acidic protein (GFAP) immunohistochemistry (IHC) ($n = 4$), terminal deoxynucleotidyl transferase dUTP nick end labeling (TUNEL) technique ($n = 4$), Western blotting (WB) ($n = 5$), or quantitative reverse transcription-polymerase chain reaction (qRT-PCR) ($n = 5$). In every case, the numbers indicate the number of rats per drug treatment. A separate group of five rats per drug treatment was used for electroretinography (ERG) studies. After performing a basal ERG, rats were subjected to the intravitreal injections of drugs and exposed to CI. A week later, a second ERG was performed. All animals received food and water *ad libitum*. Animal care was performed in accordance with the Association for Research in Vision and Ophthalmology Statement for the Use of Animals in Ophthalmic and Vision Research. The animal model of continuous illumination and the experimental procedure were approved by the Institutional Committee for the Use and Care of Laboratory Animals of the

TABLE 1 | List of primers.

Gene	Primer orientation	Primer sequence
TNF- α	Forward	GAGAGATTGGCTGCTGGAAC
	Reverse	TGGAGACCATGATGACCGTA
IL-1 β	Forward	CCTCTGCCAAGTCAGGTCTC
	Reverse	GAATGTGCCACGGTTTTCTT
GFAP	Forward	GAAGAAAACCGCATCACCAT
	Reverse	GGCACACCTCACATCACATC
iNOS	Forward	AGGCCACCTCGGATATCTCT
	Reverse	GCTTGTCTCTGGGTCTCTG
18 S	Forward	ATGCTCTTAGCTGAGTGTCCCG
	Reverse	ATTCTAGCTGCGGTATCCAGG

Facultad de Medicina, Universidad de Buenos Aires (CICUAL, Res (CD) 3130/2017).

Tissue Processing for Immunohistochemistry and Terminal Deoxynucleotidyl Transferase dUTP Nick End Labeling Assay

Eyes containing the retinas were fixed by immersion in a 4% paraformaldehyde solution for 24 h. After cryoprotection in a 30% sucrose solution, the eyes were embedded in gelatine, blocks were frozen, and sections were obtained using a Lauda Leitz cryostat. Sections (thickness: 20 μm) were mounted on gelatine-coated glass slides and processed by IHC or TUNEL techniques.

Immunohistochemistry Technique

Endogenous peroxidase activity was inhibited by incubation in methanol containing 3% hydrogen peroxide for 30 min. Overnight incubation with GFAP polyclonal primary antibody (Dako Ink, Cat #Z0334, United States, dilution 1:500) was performed at 4°C. Then sections were incubated with biotinylated goat anti-rabbit antibody (Sigma Chemical Co., MO; Cat #B8895, dilution 1:500) at room temperature (RT) for 1 h followed by ExtrAvidin-Peroxidase[®] complex (Sigma Chemical Co., MO., United States; Cat E2886, dilution 1:500) at room temperature (RT) for 1 h as well. Development was performed using the DAB/nickel intensification procedure (Hancock, 1984). Controls were performed by omitting primary antibodies.

Terminal Deoxynucleotidyl Transferase dUTP Nick End Labeling Assay

Cryostat sections were processed using the ApopTag Peroxidase *In Situ* kit (Chemicon Int, CA, United States, S701), following the instructions described in Soliño et al. (2018). Briefly, sections were incubated with terminal deoxynucleotidyl transferase (Chemicon Int, CA, United States, Cat 90,418) (1 h at 37°C) followed by the anti-digoxigenin conjugate

(Chemicon Int, CA, United States, Cat 90,420) (30 min at RT). The reaction was developed using the diaminobenzidine/nickel intensification procedure, and sections were counterstained with eosin.

Image Analysis of Terminal Deoxynucleotidyl Transferase dUTP Nick End Labeling and Glial Fibrillary Acidic Protein Immunostained Sections

Six retinal sections of both eyes from each experimental group were analyzed (CGS21680, $n = 4$; SCH58261, $n = 4$). Anatomically matched areas of retina among animals were selected, and images were taken using a Zeiss Axiophot microscope attached to a video camera (Olympus Q5) under the same light conditions (Soliño et al., 2018).

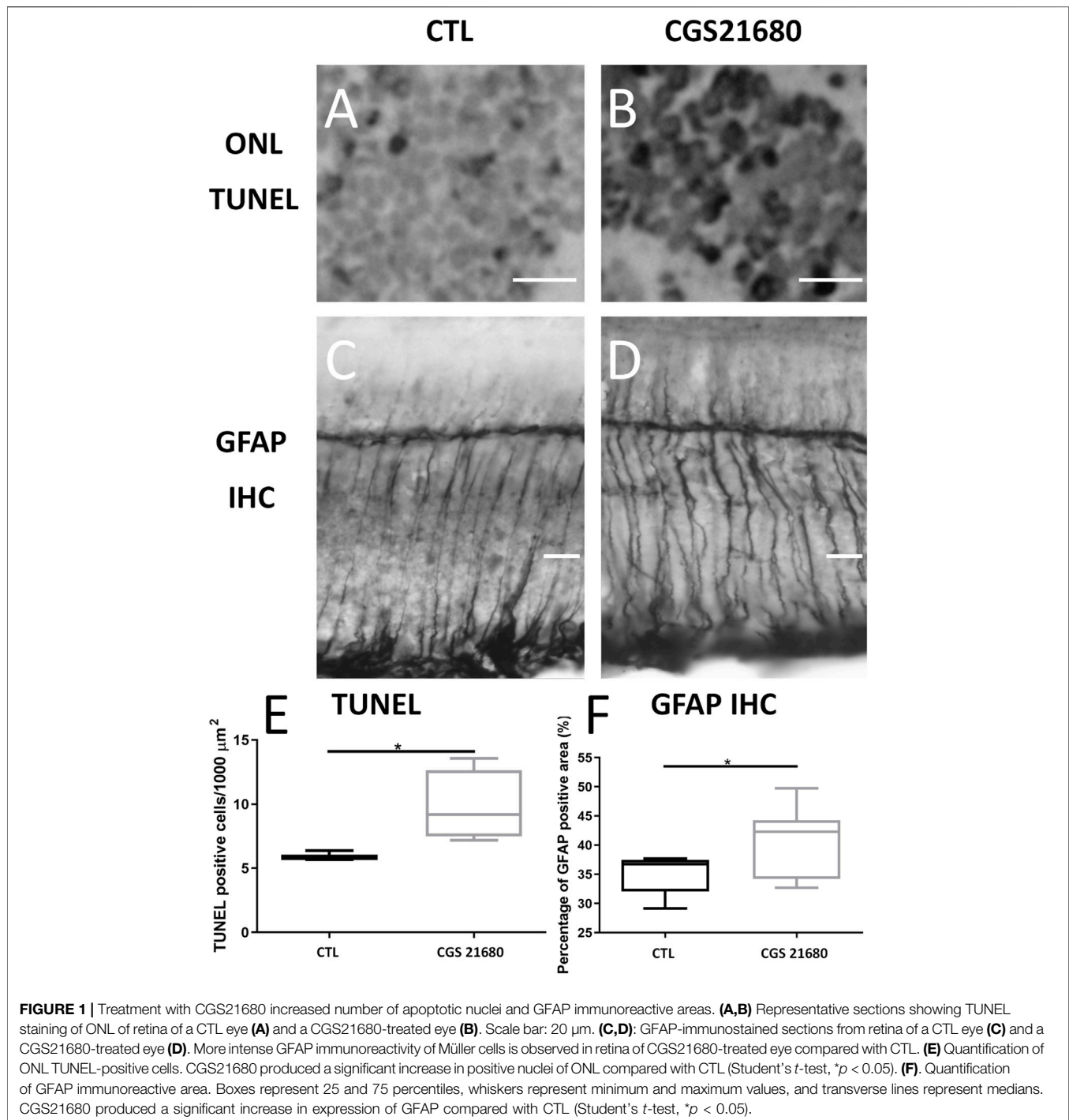
The following parameters were measured, blind to treatment, on 8-bit images, using the Fiji software (NIH, Research Services Branch, National Institutes of Mental Health, Bethesda, MD, United States):

GFAP-positive area: Images of drug-treated and control retinas were randomly selected. The immunoreactive area of the whole section was thresholded. The region of interest (ROI) was the retinal surface between the two limiting membranes where Müller cells extend their processes. The GFAP-positive area was calculated as the percentage of the ROI immunostained by GFAP.

TUNEL positive nuclei/1,000 μm^2 : Images of drug-treated and control retinas were randomly selected and thresholded. As for ROI, frames of 1,000 μm^2 were randomly determined on the outer nuclear layer (ONL) of treated and control retinas. The analyzed particles function of Fiji was used (Grishagin, 2015), and the TUNEL positive nuclei/1,000 μm^2 ratio was then obtained for each ROI.

Western Blotting

The procedure was performed as previously described in Soliño et al. (2018). Retinas were homogenized (1:3, w/v) in lysis buffer (100 mM NaCl, 10 mM Tris-HCl, 0.5% Triton X-100) plus 50 μl of protease inhibitor cocktail (Merck KGaA, Darmstadt, Germany) at 4°C. Protein concentration was determined by the Bradford method. Then, 25 μg of each sample were mixed 4:1 with 5 \times sample buffer (10% sodium dodecyl sulfate, 0.315-M Tris-HCl, 25% beta-mercaptoethanol, 50% glycerol, 0.2-ml bromophenol blue 0.1%, pH 6.8), separated by 15% sodium dodecyl sulfate–polyacrylamide gel electrophoresis and transferred to polyvinylidene difluoride membranes (GE Healthcare Life Sciences, IL, United States). Kaleidoscope Prestained Standards (Bio-Rad Laboratories, CA, United States) were used as molecular weight markers. Membranes were blocked with phosphate-buffered saline/5% nonfat dry milk and incubated overnight at 4°C with either a rabbit polyclonal antibody to GFAP (DAKO Inc., CA, United States, Cat Z0334; dilution 1:500) or a rabbit polyclonal antibody to activated caspase-3 (Sigma Chemical Co., MO., United States; Cat H277. dilution 1:



100) and reprobed with a monoclonal anti- β -actin antibody (Sigma Chemical Co., MO, United States, CaT C8487, dilution: 1: 1,000). Membranes were incubated with Amersham ECL donkey anti-rabbit IgG, HRP-linked F (ab) 2 fragment, Cat GENA9340, and were developed using a chemiluminescence kit (SuperSignal West Pico Chemiluminescent Substrate, Thermo Scientific, MA, United States, Cat # 34,079). Membranes were exposed to X-ray blue films (Agfa Healthcare, Argentina), which

were developed and then scanned with an HP Photosmart scanner. Optical density was quantified using Image Studio Light software. The results were normalized against β -actin.

Electroretinography

After overnight dark adaptation, rats were anesthetized under dim red illumination with ketamine and xylazine, as was mentioned earlier. An ophthalmic solution containing 5%

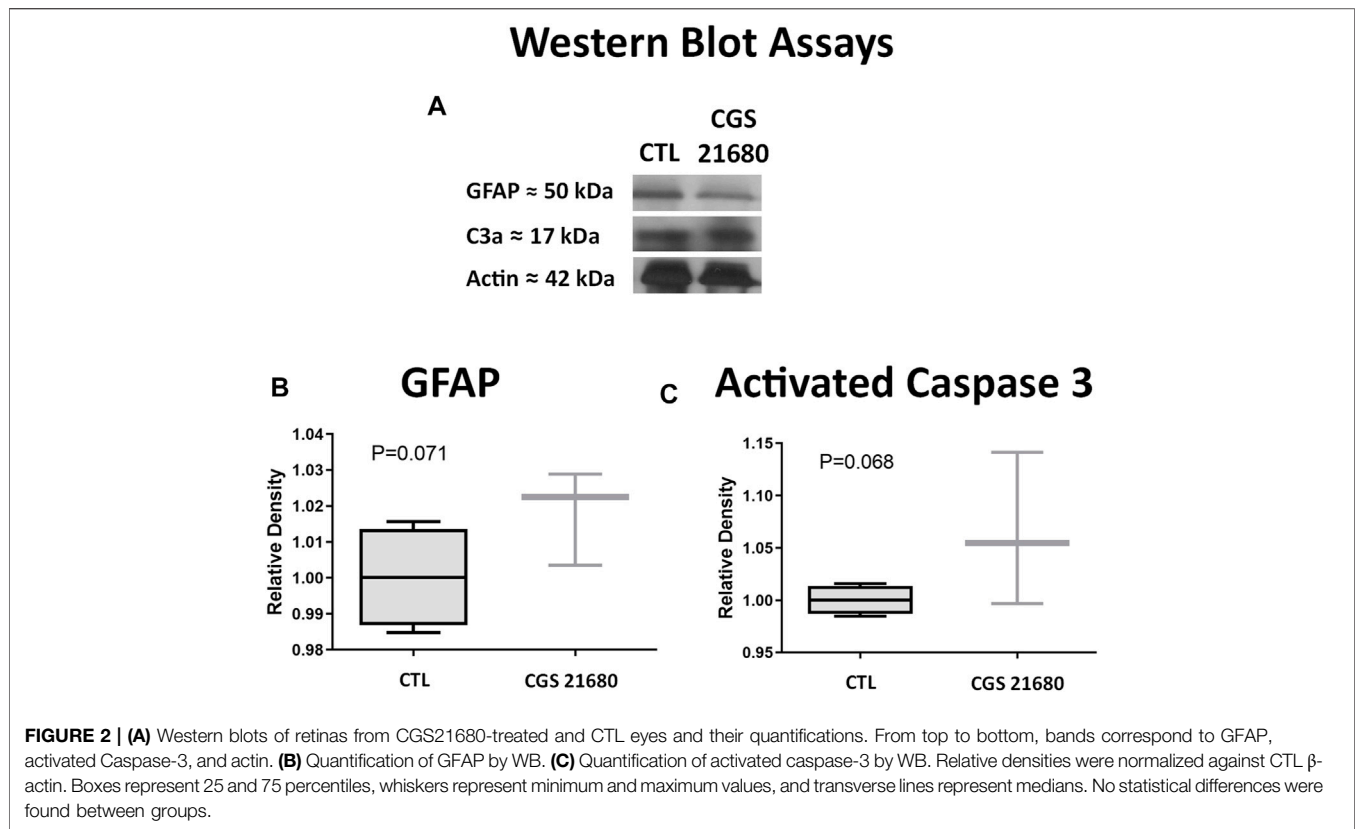


TABLE 2 | ERG recordings of eyes treated with CGS21680 and their controls. Mean values and standard deviations are shown. No statistical differences were found between groups.

	Control		CGS 21680	
	Basal	7 days Post-CI	Basal	7 days Post-CI
a-Wave (μV)	3.68 ± 1.88	8.28 ± 6.2	4.64 ± 1.71	10.25 ± 6.91
b-Wave (μV)	99.27 ± 41.82	46.53 ± 23.46	120.9 ± 60.93	60.48 ± 30.19
OP (μV)	37.05 ± 18.11	9.15 ± 5.71	42.71 ± 21.51	11.74 ± 5.71

phenylephrine hydrochloride and 0.5% tropicamide (Fotorretin, Laboratorios Poen, Argentina) was used to dilate the pupils. Recordings were made from both eyes simultaneously (Soliño et al., 2018).

Scotopic ERG: 20 responses to flashes of white light (1 ms, 1 Hz) from a photic stimulator (light-emitting diodes) set at maximum brightness were recorded with an Akonic BIO-PC electroretinograph (Argentina). The registered response was amplified and filtered (1.5-Hz low-pass filter, 500-Hz high-pass filter, notch activated).

Oscillatory potentials (OP): The same photic stimulator was used with filters of high (300 Hz) and low (100 Hz) frequencies. The amplitudes of the OPs were estimated following described methodology (Severns et al., 1994).

The a- and b-waves and OP were measured 40 times, and the values from each eye were averaged. The resultant mean values were used to obtain the group

means of a- and b-waves and OP amplitudes ± standard deviation.

RNA Isolation and Quantitative Reverse Transcription-Polymerase Chain Reaction

The retinas were processed as detailed in Soliño et al. (2018). Briefly, tissues were homogenized with TRIzol (Invitrogen, Madrid, Spain), and RNA was isolated with RNeasy Mini kit (Qiagen, Germantown, MD, United States). Three micrograms of total RNA were treated with 0.5-μl DNaseI (Invitrogen) and reverse-transcribed into first-strand copy DNA using random primers and the SuperScript III kit (Invitrogen). Reverse transcriptase was omitted in control reactions. The resulting copy DNA was mixed with SYBR Green PCR master mix (Invitrogen) for qRT-PCR using 0.3 μM forward and reverse oligonucleotide primers (see Table 1). Quantitative measures

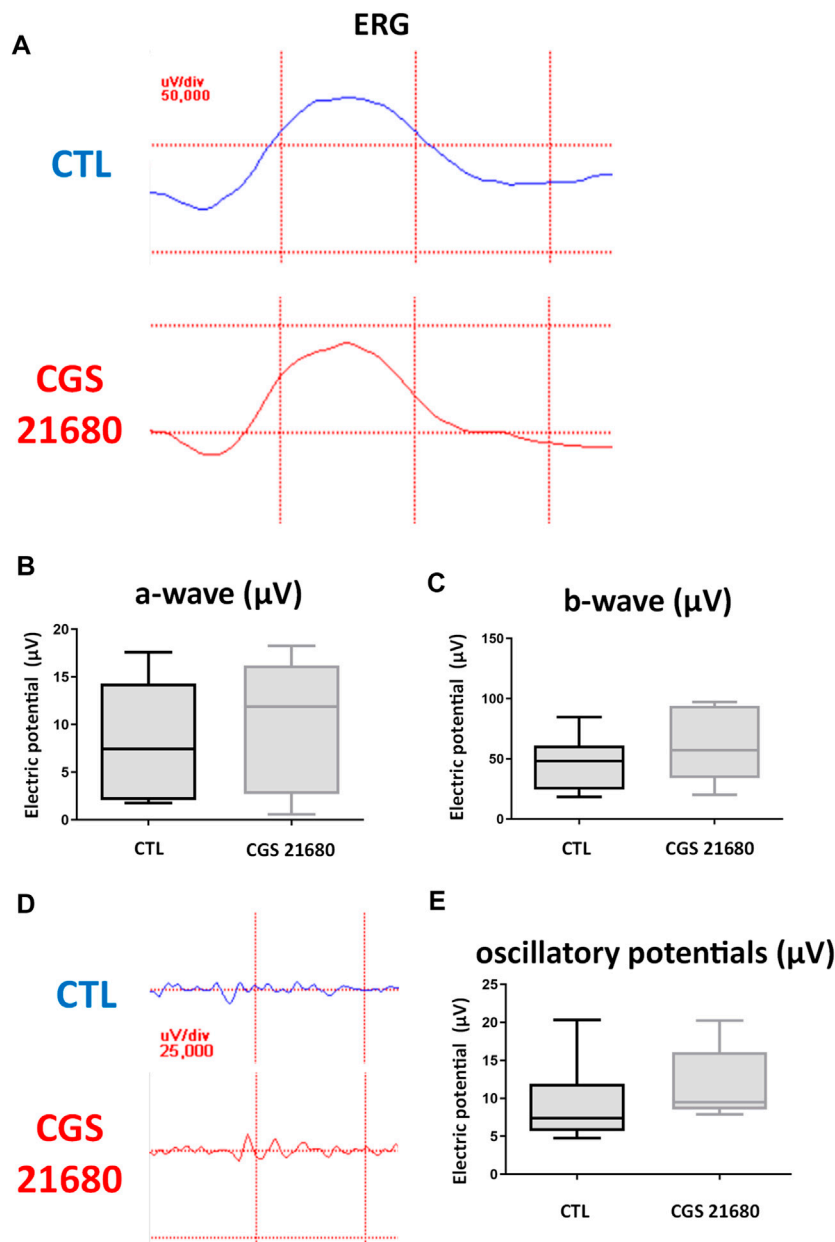
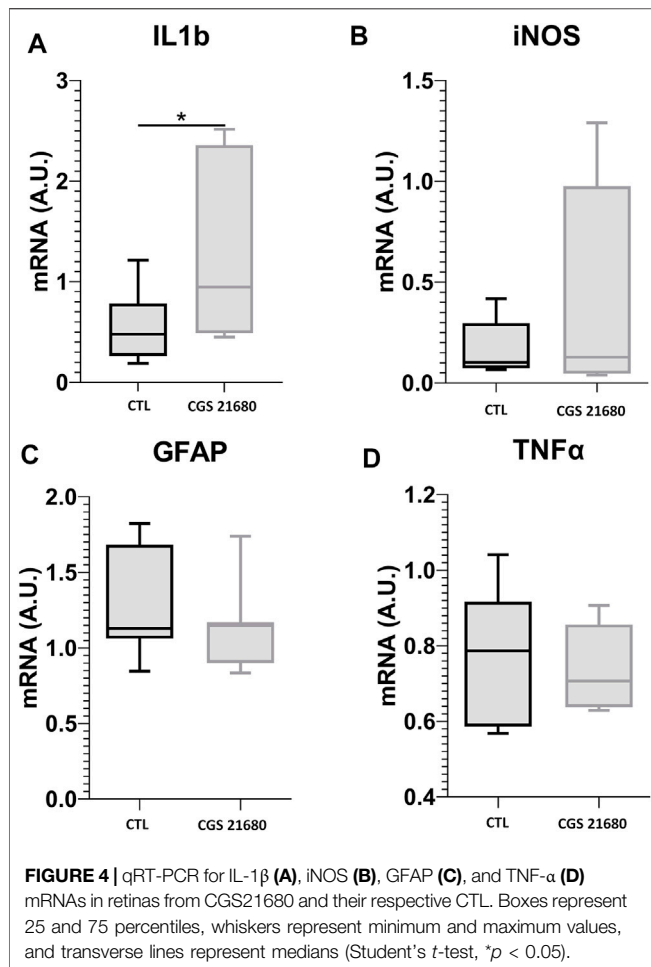


FIGURE 3 | ERG recordings of control eyes (CTL) and CGS21680-treated eyes. **(A)** ERG recording a CTL eye (above) and a CGS21680-treated eye (below) 1 week after CI. **(B)** Quantification of a-wave. **(C)** Quantification of b-wave. **(D)** Response of oscillatory potentials 1 week after exposure to CI of a CTL eye (above) and an eye treated with CGS21680 (below). **(E)** Quantifications of OP. Boxes represent 25 and 75 percentiles, whiskers represent minimum and maximum values, and transverse lines represent medians. No statistical differences were found between groups.

were performed using a 7,300 Real-Time PCR System (Applied Biosystems, Carlsbad, CA, USA). Cycling conditions were an initial denaturation at 95°C for 10 min, followed by 40 cycles of 95°C for 15 s and 60°C for 1 min. At the end, a dissociation curve was implemented from 60 to 95°C to validate amplicon specificity. Gene expression was calculated using relative quantification by interpolation into a standard curve. All values were divided by the expression of the housekeeping gene 18S.

Statistical Analysis

D'Agostino, KS, Shapiro-Wilk, and F tests confirmed that the data of image analysis of GFAP, IHC, and TUNEL studies of CGS21680-treated rats ($n = 4$) and SCH 58261-treated rats ($n = 4$) display a Gaussian distribution. Then, all the data of this study [GFAP-IHC ($n = 4$), TUNEL ($n = 4$), WB ($n = 5$), qRT-PCR ($n = 5$), and ERG ($n = 5$)] were analyzed using unpaired Student's *t*-test (GraphPad Software, San Diego, CA, United States). In every case, *n* is the number of animals per drug treatment. Values



are expressed as mean \pm standard deviation. Differences were considered significant when *p* < 0.05.

The sample size was calculated based on data published by Soliño et al. (2018). In that study, the number of apoptotic cells, as quantified by TUNEL analysis, was 4.25 positive nuclei/1,000 μm^2 in animals subjected to LIRD and was reduced to 1.45 when subjects were treated with N6-cyclopentyladenosine, with a standard deviation of 0.74. Free software (<http://biomath.info/power/ttest.htm>) was used to calculate the sample size. Power was set as 80% for an alpha of 5%, resulting in less than six animals per group to reach a significant improvement of the variable with an unpaired *t*-test.

RESULTS

Effects of the Administration of CGS21680 Before Light-Induced Retinal Degeneration Effects on Photoreceptor Apoptosis and Gliosis

In the sections stained with the TUNEL technique, a greater density of positive nuclei was observed in the ONL of the retina of CGS21680-treated eyes (9.78 ± 2.752 vs. 5.974 ± 0.3612 , *p* < 0.05, *n* = 4) (Figures 1A,B,E and Supplementary Figure S3).

The retinas of CGS21680-treated eyes showed an increase GFAP immunoreactivity ($40.57 \pm 5.948\%$ vs. $35.18 \pm 3.518\%$, *p* < 0.05) (Figures 1C,D,F).

Apoptosis and Glial Reactivity After Administration of CGS21680

No significant differences were seen in protein expression of GFAP and activated caspase-3 between the retinas of eyes treated with CGS21680 and CTL (Figure 2 and Supplementary Figure S4).

Electroretinography After Administration of CGS21680

The eyes treated with CGS21680 did not show significant differences in any of the studied parameters between treated eyes 7 days post-illumination and control eyes 7 days post-illumination: a-wave (*p* = 0.27), b-wave (*p* = 0.19), and oscillatory potentials (*p* = 0.22, Table 2 and Figure 3).

Effects of CGS21680 on Gene Expression (Quantitative Reverse Transcription-Polymerase Chain Reaction)

To investigate the mechanism of action of the A2AR agonist, CGS21680, we studied the expression of genes involved in cell damage and inflammation. qRT-PCRs of the retinas were performed after the treatment with CGS21680, followed by 24 h of CI. Cytokine IL-1 β expression increased significantly (1.278 ± 0.9059 vs. 0.5573 ± 0.3511 ; *p* < 0.05) (Figure 4A), whereas inducible nitric oxide synthase (iNOS) messenger RNA (mRNA) and TNF- α mRNA did not change significantly (Figures 4B,D). The astroglial marker, GFAP mRNA, did not change after treatment with CGS21680 (Figure 4C).

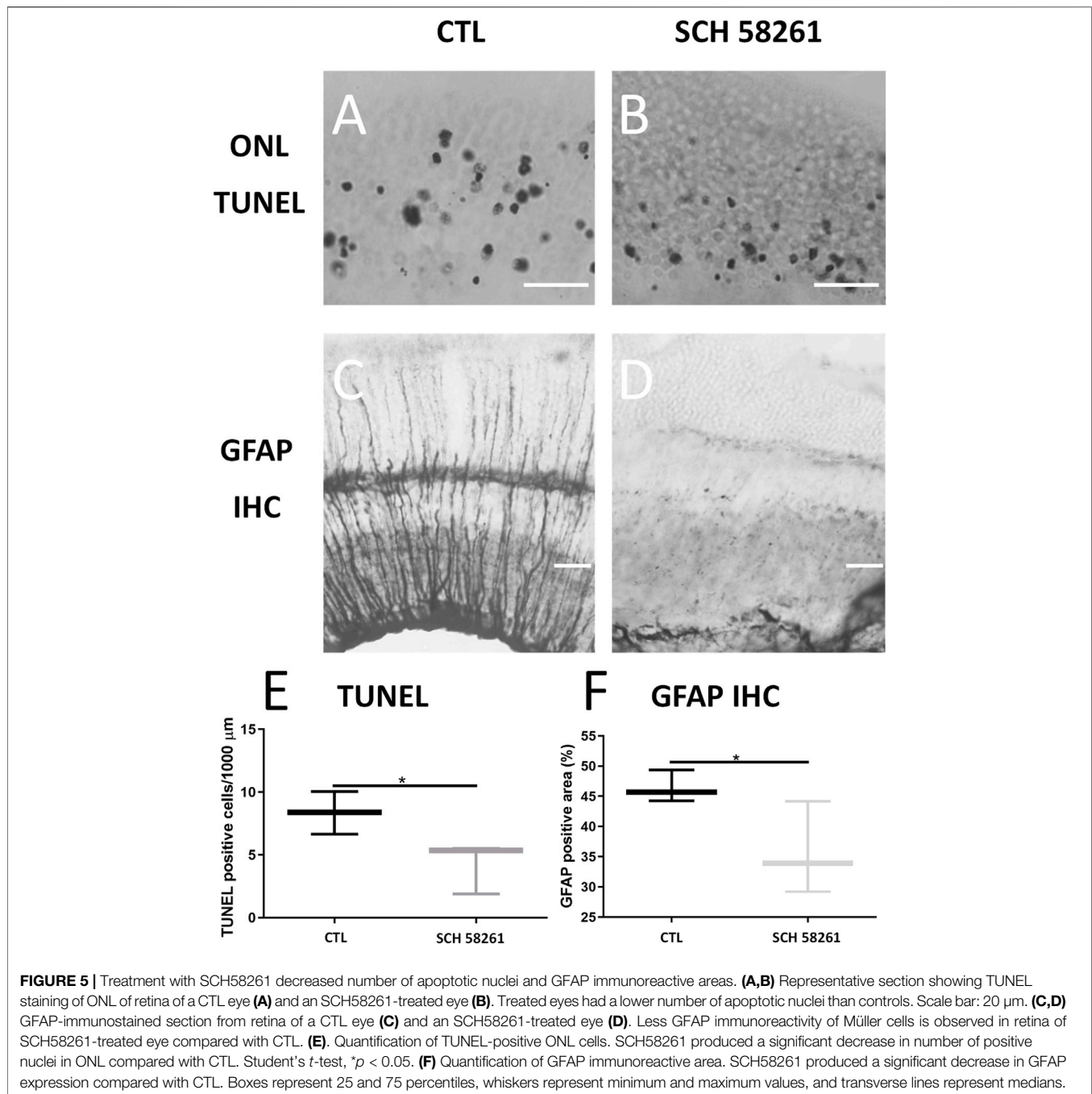
Effects of the Administration of SCH58261 Before Light-Induced Retinal Degeneration Effects on Photoreceptor Apoptosis and Gliosis

TUNEL staining showed that the number of positive nuclei decreased in SCH58261-treated eyes, indicating a lower number of apoptotic photoreceptors (8.354 ± 1.701 vs. 4.247 ± 2.056 , *p* < 0.05) (Figures 5A,B,E and Supplementary Figure S3).

The quantification of GFAP immunoreactivity showed the reduction of GFAP-immunostained areas in the retinas of SCH58261-treated eyes, demonstrating less glial activation ($35.76 \pm 7.625\%$ vs. $46.44 \pm 2.643\%$, *p* < 0.05). (Figures 5C,D,F).

Effects of SCH58261 on Apoptosis and Glial Reactivity by Western Blot

Changes in the levels of activated caspase-3 and GFAP are in agreement with previous TUNEL and IHC results. A significant decrease of GFAP levels in the treated eyes was found (0.5477 ± 0.09308 vs. 1 ± 0.06348 , *p* < 0.01) (Figures 6A,C and Supplementary Figure S4). Also, a statistically significant decrease in activated caspase-3 levels in the retinas of SCH58261-treated eyes was confirmed (0.7853 ± 0.1611 vs. 1 ± 0.030220 , *p* < 0.05) (Figures 6B,D and Supplementary Figure S4).



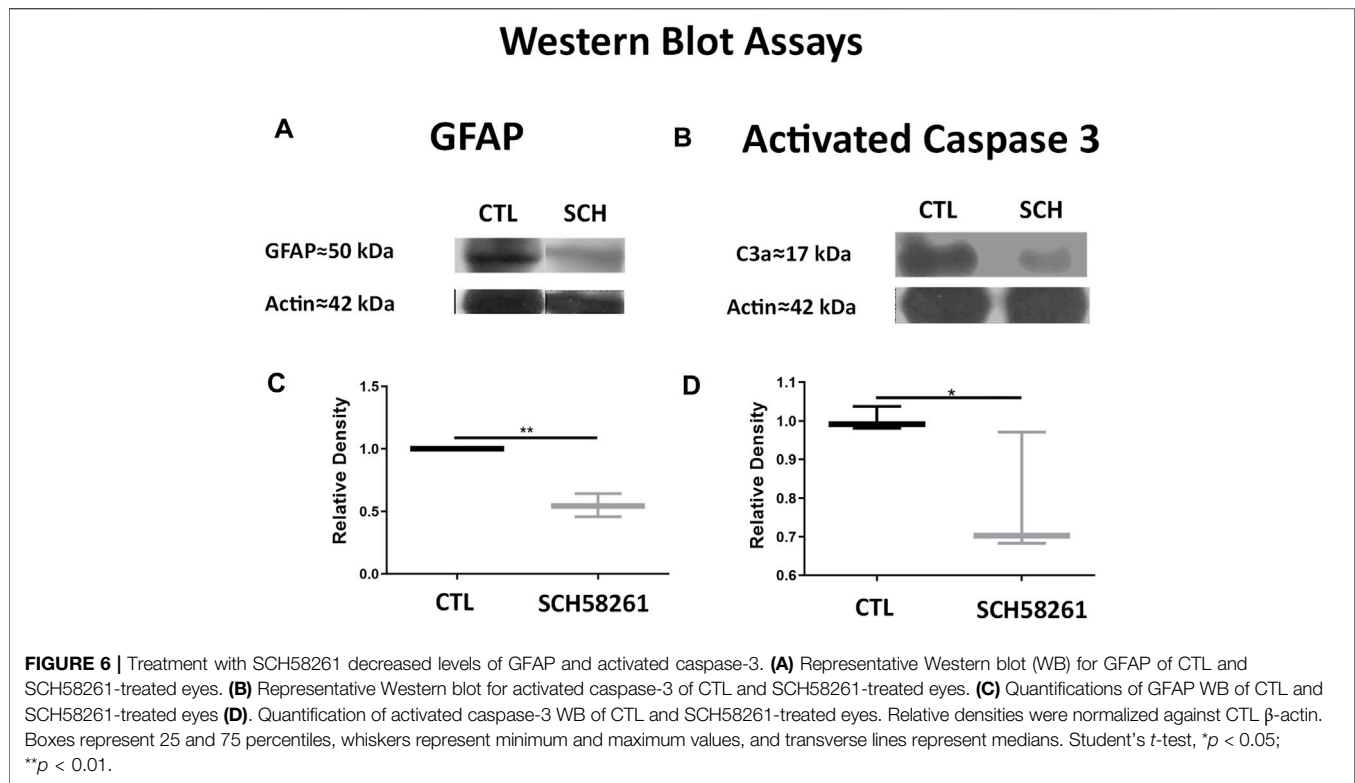
Effects of SCH58261 on Retinal Function Determined by Electrophysiology

SCH58261-treated eyes showed a greater response of the photoreceptors as larger a-wave was recorded compared with CTL eyes ($p < 0.05$) (Figures 7A,B; Table 3).

Also, the function of the inner retina was protected, as the amplitude of the b-wave and OP was significantly larger in SCH58261-treated eyes compared with CTL eyes ($p < 0.05$ in both cases) (Figures 7C–E; Table 3).

Effects of SCH58261 on Gene Expression (Quantitative Reverse Transcription-Polymerase Chain Reaction)

Similarly, to investigate the neuroprotective mechanism of the A2AR antagonist SCH58261, we studied the expression of genes involved in cell damage and inflammation. qRT-PCRs of the retinas were performed after the treatment with SCH58261, followed by 24 h of CI. TNF- α decreased significantly in SCH58261-treated retinas (1.089 ± 0.1431 vs. 1.271 ± 0.2668 ,



p < 0.01) (**Figure 8D**), whereas the expression of cytokine IL-1 β , iNOS, and GFAP did not change significantly (**Figures 8A–C**).

DISCUSSION

Results presented herein indicated that an A2AR agonist (CGS21680) exacerbated the damage induced by light exposure to the retina. CGS21680-treated eyes presented higher densities of apoptotic nuclei in ONL and higher glial reactivity, evidenced by an increase of the GFAP immunoreactive area. However, the WB study did not confirm these data, and functional studies using ERG showed no differences between treated eyes and their CTL. This phenomenon could be explained because CI produced such functional damage that it cannot be worsened by an A2AR agonist. Also, it may be speculated that the techniques used to detect apoptosis (TUNEL) and GFAP immunohistochemistry have greater sensitivity to detect damage at the cellular level than the WB of the full retinal tissue. Alternatively, it must be mentioned that there are strong pharmacological arguments in brain tissue questioning the selectivity of CGS21680, as it could also act as an agonist for the A1 receptor (Zhang et al., 1994; Cunha et al., 1996; Cunha et al., 1999). This could also be the reason underlying the lack of effect of this drug.

On the opposite, we found that a lower A2AR activity due to an antagonist intravitreal injection was protective to the retina, as SCH58261-treated retinas showed smaller amounts of apoptotic nuclei in ONL and lower glial reactivity. Both data were confirmed by WB because SCH58261-treated retinas had lower levels of

activated caspase-3 and GFAP. Finally, SCH 58261 also protected the retinal function, as all ERG parameters were preserved.

It was demonstrated that A2AR inhibitors provide important protective mechanisms in the CNS, as low concentrations of adenosine activate A1R and inhibit the release of excitatory amino acids, but higher concentrations of adenosine activate A2AR and block A1R through a receptor–receptor allosteric trans-inhibition (Ciruela et al., 2006).

The role of adenosine in the inflammatory response to retinal injury is well known, and it was reported that SCH58261 protects from photoreceptor loss because it prevents the upregulation of proinflammatory mediators and the alterations of the complement system in microglial cells (Madeira et al., 2018). Also, KW6002, another A2AR antagonist, reduced the inflammatory microglial response and protected the retina from ischemic injury and reperfusion (Boia et al., 2017). Caffeine, an unspecific A2AR antagonist, was neuroprotective, as it lowered intraocular pressure and reduced the activation of microglia and the inflammatory cytokines IL-1 β and TNF- α in a mouse glaucoma model (Madeira et al., 2016b). To investigate the neuroprotective mechanism of the A2AR antagonist, we studied the expression of genes involved in inflammation and cell damage by qRT-PCR, and we found that SCH58261 lowered the levels of TNF- α expression, supporting the idea that it reduces the upregulation of inflammatory microglial mediators. This lower inflammatory milieu could favor the survival of the photoreceptors and could allow the conservation of the function.

The observed neuroprotective effect of A2AR antagonism in LIRD is aligned with the neuroprotective effect of chronic caffeine intake (Cunha and Agostinho, 2010) and with

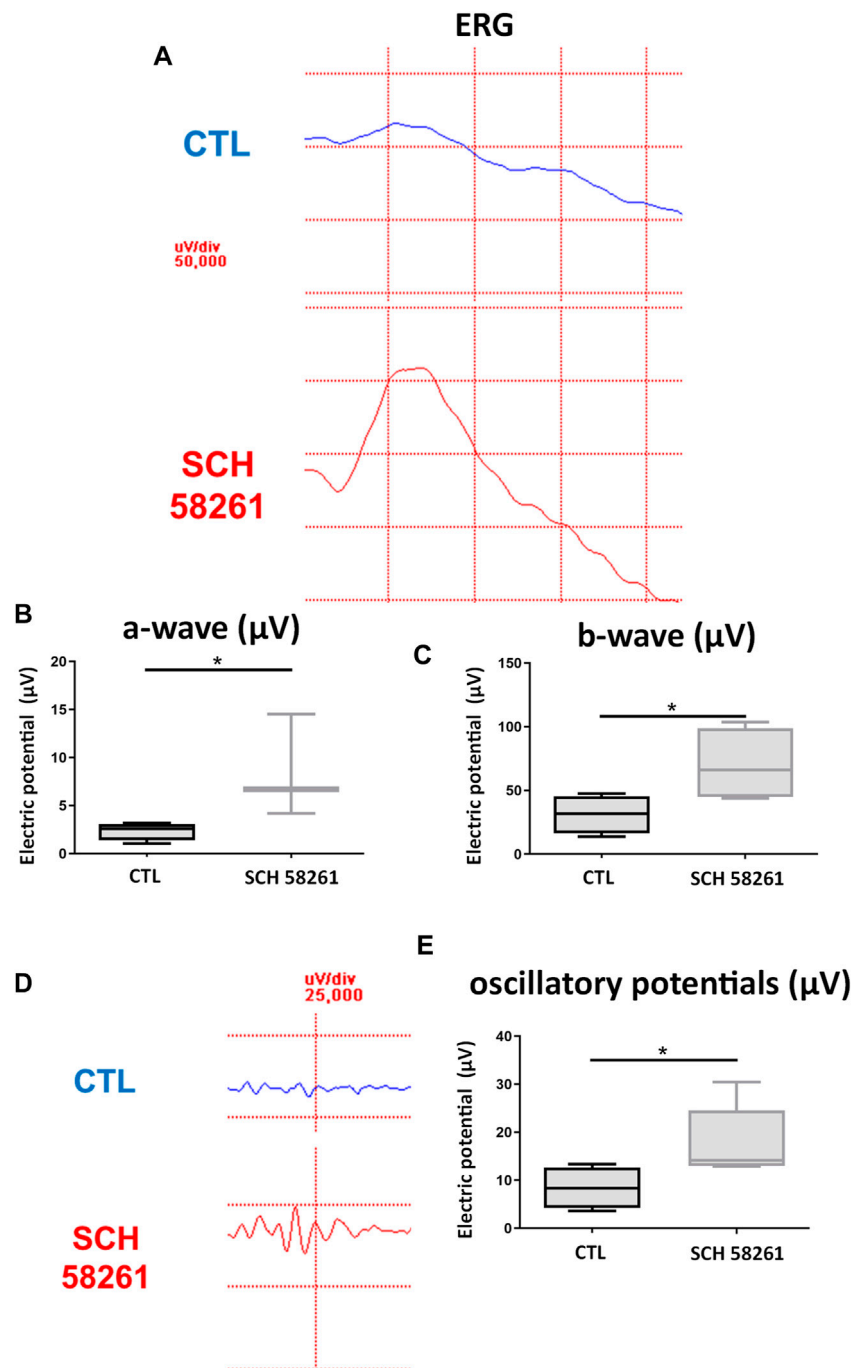


FIGURE 7 | Effect of treatment with SCH58261 on ERG recordings post CI. **(A)** ERG recording 1 week after exposure to 24 h of CI of a CTL eye (above) and an SCH58261-treated eye (below). **(B)** Quantification of a-wave. **(C)** Quantification of b-wave. **(D)** Response of oscillatory potentials 1 week after 24 h of CI of a CTL eye (above) and an SCH58261-treated eye (below). **(E)** Quantification of OP. Boxes represent 25 and 75 percentiles, whiskers represent minimum and maximum values, and transverse lines represent medians. Student's *t*-test, **p* < 0.05.

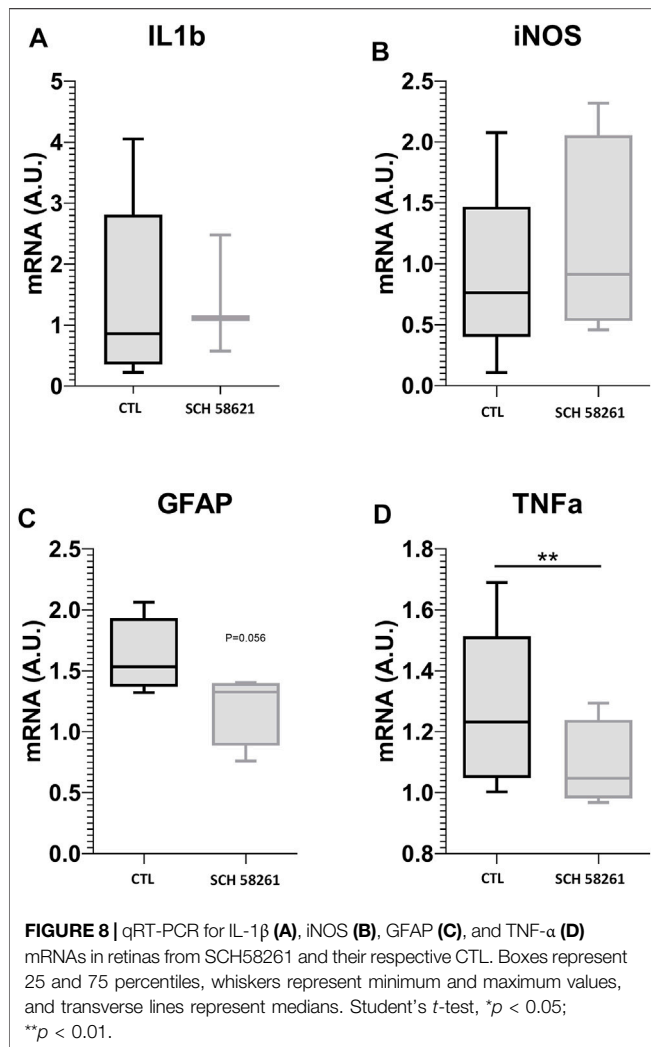
caffeine reduction of apoptosis in oxygen-induced retinopathy (Zhang et al., 2017).

On the contrary, using two different models of perinatal brain injury, CGS21680 produced a partial increase of some microglial cytokines such as IL-1 β and TNF- α , as well as an increase of iNOS

(Colella et al., 2018). In agreement with this, in our model of CI, CGS21680 produced a similar phenomenon, as we also detected an increase of the cytokine IL-1 β . Surprisingly, no significant effects were observed in iNOS and TNF- α mRNA expression.

TABLE 3 | ERG recordings and oscillatory potentials of eyes treated with SCH58261 and their controls. Mean values and standard deviations are shown, Student's *t*-test, **p* < 0.05.

	Control		SCH 58261	
	Basal	Post-CI	Basal	Post-CI
a-Wave (μV)	4.62 ± 3.56	2.35 ± 0.92	4.84 ± 4.40	8.46 ± 5.39*
b-Wave (μV)	99.79 ± 50.97	31.23 ± 14.98	99.02 ± 52.35	69.98 ± 28.88*
OP (μV)	33.27 ± 10.35	8.405 ± 4.363	37.59 ± 15.17	17.83 ± 7.41*



Herein, we detected lower levels of Müller glia activation in SCH58261-treated eyes, suggesting that modulation by A2AR may be involved in the inflammatory reaction. This finding is in line with the observation that the injection of antagonist SCH 442416 reverses the changes in the expression of channels and transporters in Müller cells responsible for maintaining retinal homeostasis (Yang et al., 2015).

Although the role of A2AR antagonist on microglial inflammation seems to be the main mechanism involved in the protection of the retina, we postulate that a direct neuroprotective

effect on the photoreceptors themselves cannot be ruled out, as A2 receptors are localized in rabbit and mouse outer retinas (Blazynski, 1990; Blazynski and Perez, 1991), and A2AR was also found in the photoreceptors of different species (McIntosh and Blazynski, 1994; Rey and Burnside, 1999; Stella et al., 2002; Li et al., 2014). Further studies are needed to confirm this hypothesis.

Finally, we studied the changes in the expression of the A2A receptor. CGS 21680 produced no significant changes (Supplementary Figure S1), but SCH 58261 produced a significant reduction in the expression of the receptor (Supplementary Figure S2). This would increase the antagonistic effects of SCH 58261 by diminishing the available receptors and may also explain the protective effect of the drug.

In summary, this study shows that the blockade of A2A receptors before exposure to continuous light prevents retina damage and preserves retinal function by lowering inflammation, glial reactivity, and apoptosis in ONL. These results allow us to postulate that the modulation of A2AR activity may be a strategy that deserves to be evaluated in degenerative pathologies of the retina.

DATA AVAILABILITY STATEMENT

The original contributions presented in the study are included in the article/Supplementary Material; further inquiries can be directed to the corresponding author.

ETHICS STATEMENT

The animal study was reviewed and approved by Comité Institucional para el Cuidado y Uso de Animales de Laboratorio (CICUAL), Facultad de Medicina, Universidad de Buenos Aires [CICUAL, Res (CD) 3130/2017].

AUTHOR CONTRIBUTIONS

MS and IL made most of the experimental work. EL, MB, CL, and EG helped with IHC and WB. MR-F and MS performed ERGs. AM and JL-C designed experiments, interpreted results, and wrote the paper.

FUNDING

This work was supported with grants of the University of Buenos Aires given to JL-C (UBACYT 2014-17/20020130100675BA and

2018/20020170100493BA). JL-C was the director of the lab in BA, where animals were illuminated, and IHC, WB, and ERGs were carried out. This research was funded in part by a grant (PI19/01805) from the Instituto de Salud Carlos III, co-funded by European Regional Development Fund (ERDF) “A way to build Europe”. IML was supported by Miguel Servet contracts (CP15/00198 and CPII20/00029) from the Instituto de Salud Carlos III, co-funded by European Social fund (ESF) “Investing in your future” and by the Fundación Rioja Salud (FRS) given to AM. AM was the director of the Spanish lab where qRT-PCRs were carried out.

SUPPLEMENTARY MATERIAL

The Supplementary Material for this article can be found online at: <https://www.frontiersin.org/articles/10.3389/fphar.2022.840134/full#supplementary-material>

REFERENCES

- Blazynski, C. (1990). Discrete Distributions of Adenosine Receptors in Mammalian Retina. *J. Neurochem.* 54, 648–655. doi:10.1111/j.1471-4159.1990.tb01920.x
- Blazynski, C., and Perez, M. T. (1991). Adenosine in Vertebrate Retina: Localization, Receptor Characterization, and Function. *Cell Mol Neurobiol.* 11, 463–484. doi:10.1007/BF00734810
- Boeck, C. R., Kroth, E. H., Bronzatto, M. J., and Vendite, D. (2005). Adenosine Receptors Co-operate with NMDA Preconditioning to Protect Cerebellar Granule Cells against Glutamate Neurotoxicity. *Neuropharmacology* 49, 17–24. doi:10.1016/j.neuropharm.2005.01.024
- Boia, R., Elvas, F., Madeira, M. H., Ares, I. D., Rodrigues-Neves, A. C., Tralhao, P., et al. (2017). Treatment with A2A Receptor Antagonist KW6002 and Caffeine Intake Regulate Microglia Reactivity and Protect Retina against Ischemia Damage. *Cell Death Dis* 8 (10), e3065. doi:10.1038/cddis.2017.451
- Canas, P. M., Porciúncula, L. O., Cunha, G. M., Silva, C. G., Machado, N. J., Oliveira, J. M., et al. (2009). Adenosine A2A Receptor Blockade Prevents Synaptotoxicity and Memory Dysfunction Caused by Beta-Amyloid Peptides via P38 Mitogen-Activated Protein Kinase Pathway. *J. Neurosci.* 29, 14741–14751. doi:10.1523/JNEUROSCI.3728-09.2009
- Ciruela, F., Casadó, V., Rodrigues, R. J., Luján, R., Burgueño, J., Canals, M., et al. (2006). Presynaptic Control of Striatal Glutamatergic Neurotransmission by Adenosine A1-A2a Receptor Heteromers. *J. Neurosci.* 26, 2080–2087. doi:10.1523/JNEUROSCI.3574-05.2006
- Colella, M., Zinni, M., Pansiot, J., Cassanello, M., Mairesse, J., Ramenghi, L., et al. (2018). Modulation of Microglial Activation by Adenosine A2a Receptor in Animal Models of Perinatal Brain Injury. *Front. Neurol.* 9, 605. doi:10.3389/fneur.2018.00605
- Cunha, R. A. (2016). How Does Adenosine Control Neuronal Dysfunction and Neurodegeneration? *J. Neurochem.* 139, 1019–1055. doi:10.1111/jnc.13724
- Cunha, R. A., and Agostinho, P. M. (2010). Chronic Caffeine Consumption Prevents Memory Disturbance in Different Animal Models of Memory Decline. *J. Alzheimers Dis.* 20 (Suppl. 1), S95–S116. doi:10.3233/JAD-2010-1408
- Cunha, R. A., Constantino, M. D., and Ribeiro, J. A. (1999). G Protein Coupling of CGS 21680 Binding Sites in the Rat hippocampus and Cortex Is Different from that of Adenosine A1 and Striatal A2A Receptors. *Naunyn Schmiedebergs Arch. Pharmacol.* 359, 295–302. doi:10.1007/pl00005355
- Cunha, R. A., Johansson, B., Constantino, M. D., Sebastião, A. M., and Fredholm, B. B. (1996). Evidence for High-Affinity Binding Sites for the Adenosine A2A Receptor Agonist [3H] CGS 21680 in the Rat hippocampus and Cerebral Cortex that Are Different from Striatal A2A Receptors. *Naunyn Schmiedebergs Arch. Pharmacol.* 353, 261–271. doi:10.1007/BF00168627
- SUPPLEMENTARY FIGURE S1** | qRT-PCR for A2A receptor in retinas from CGS 21680 treated eyes and their respective CTL. Primers A2A: Forward CGGGAAGCTC CACGAAGACC Reverse AGCAAAGAGCCCCGACGATG. Boxes represent 25 and 75 percentiles, whiskers represent minimum and maximum values and transverse lines represent means.
- SUPPLEMENTARY FIGURE S2** | qRT-PCR for A2A receptor in retinas from SCH58261 treated eyes and their respective CTL. Primers A2A: Forward CGGGAA CTCCACGAAGACC Reverse AGCAAAGAGCCCCGACGATG. Boxes represent 25 and 75 percentiles, whiskers represent minimum and maximum values and transverse lines represent means. Student's t test, * P <0.05.
- SUPPLEMENTARY FIGURE S3** | Left. Representative section of a retina treated with SCH58261 and the corresponding control. Observe the lower number of apoptotic nuclei in ONL. Right: Representative section of a retina treated with CGS21680 and the corresponding control. PRL, photoreceptor layer; ONL, outer nuclear layer; OPL, outer plexiform layer; INL, inner nuclear layer, IPL, inner plexiform layer; GCL, ganglion cell layer. Scale bar: 20 µm.
- SUPPLEMENTARY FIGURE S4** | Top. Western blot membranes of retinas from CGS21680-treated and CTL eyes. From top to bottom, the bands correspond to activated caspase-3, GFAP and actin. B. Bottom. Western blot membranes of retinas from SCH 58261-treated and CTL eyes. From top to bottom, the bands correspond to activated Caspase-3, GFAP and actin. B.
- Dos Santos-Rodrigues, A., Pereira, M. R., Brito, R., de Oliveira, N. A., and Paes-de-Carvalho, R. (2015). Adenosine Transporters and Receptors: Key Elements for Retinal Function and Neuroprotection. *Vitam Horm.* 98, 487–523. doi:10.1016/bs.vh.2014.12.014
- Dureau, P., Bonnel, S., Menasche, M., Dufier, J. L., and Abitbol, M. (2001). Quantitative Analysis of Intravitreal Injections in the Rat. *Curr. Eye Res.* 22, 74–77. doi:10.1076/ceyr.22.1.74.6974
- Font, L., Mingote, S., Farrar, A. M., Pereira, M., Worden, L., Stopper, C., et al. (2008). Intra-accumbens Injections of the Adenosine A2A Agonist CGS 21680 Affect Effort-Related Choice Behavior in Rats. *Psychopharmacology (Berl)* 199, 515–526. doi:10.1007/s00213-008-1174-z
- Gomes, C. A., Simões, P. F., Canas, P. M., Quiroz, C., Sebastião, A. M., Ferré, S., et al. (2009). GDNF Control of the Glutamatergic Cortico-Striatal Pathway Requires Tonic Activation of Adenosine A Receptors. *J. Neurochem.* 108, 1208–1219. doi:10.1111/j.1471-4159.2009.05876.x
- Gori, M. B., and Girardi, E. (2013). 3-Mercaptopropionic Acid-Induced Repetitive Seizures Increase GluN2A Expression in Rat hippocampus: a Potential Neuroprotective Role of Cyclopropyladenosine. *Cell Mol Neurobiol.* 33, 803–813. doi:10.1007/s10571-013-9947-2
- Grishagin, I. V. (2015). Automatic Cell Counting with ImageJ. *Anal. Biochem.* 473, 63–65. doi:10.1016/j.ab.2014.12.007
- Gyoneva, S., Shapiro, L., Lazo, C., Garnier-Amblard, E., Smith, Y., Miller, G. W., et al. (2014). Adenosine A2A Receptor Antagonism Reverses Inflammation-Induced Impairment of Microglial Process Extension in a Model of Parkinson's Disease. *Neurobiol. Dis.* 67, 191–202. doi:10.1016/j.nbd.2014.03.004
- Hancock, M. B. (1984). Visualization of Peptide-Immunoreactive Processes on Serotonin-Immunoreactive Cells Using Two-Color Immunoperoxidase Staining. *J. Histochem. Cytochem.* 32, 311–314. doi:10.1177/32.3.6198359
- Housley, G. D., Bringmann, A., and Reichenbach, A. (2009). Purinergic Signaling in Special Senses. *Trends Neurosci.* 32, 128–141. doi:10.1016/j.tins.2009.01.001
- Jenner, P. (2014). An Overview of Adenosine A2A Receptor Antagonists in Parkinson's Disease. *Int. Rev. Neurobiol.* 119, 71–86. doi:10.1016/B978-0-12-801022-8.00003-9
- Kaster, M. P., Machado, N. J., Silva, H. B., Nunes, A., Ardaís, A. P., Santana, M., et al. (2015). Caffeine Acts through Neuronal Adenosine A2A Receptors to Prevent Mood and Memory Dysfunction Triggered by Chronic Stress. *Proc. Natl. Acad. Sci. U S A.* 112, 7833–7838. doi:10.1073/pnas.1423088112
- Leibovich, S. J., Chen, J. F., Pinhal-Enfield, G., Belem, P. C., Elson, G., Rosania, A., et al. (2002). Synergistic Up-Regulation of Vascular Endothelial Growth Factor Expression in Murine Macrophages by Adenosine A(2A) Receptor Agonists and Endotoxin. *Am. J. Pathol.* 160, 2231–2244. doi:10.1016/S0002-9440(10)61170-4

- Li, B., Rosenbaum, P. S., Jennings, N. M., Maxwell, K. M., and Roth, S. (1999). Differing Roles of Adenosine Receptor Subtypes in Retinal Ischemia-Reperfusion Injury in the Rat. *Exp. Eye Res.* 68, 9–17. doi:10.1006/exer.1998.0573
- Li, H., Chuang, A. Z., and O'Brien, J. (2014). Regulation of Photoreceptor gap junction Phosphorylation by Adenosine in Zebrafish Retina. *Vis. Neurosci.* 31, 237–243. doi:10.1017/S095252381300062X
- Madeira, M. H., Boia, R., Elvas, F., Martins, T., Cunha, R. A., Ambrósio, A. F., et al. (2016a). Selective A2A Receptor Antagonist Prevents Microglia-Mediated Neuroinflammation and Protects Retinal Ganglion Cells from High Intraocular Pressure-Induced Transient Ischemic Injury. *Transl. Res.* 169, 112–128. doi:10.1016/j.trsl.2015.11.005
- Madeira, M. H., Ortin-Martinez, A., Nadal-Nicolas, F., Ambrósio, A. F., Vidal-Sanz, M., Agudo-Barruso, M., et al. (2016b). Caffeine Administration Prevents Retinal Neuroinflammation and Loss of Retinal Ganglion Cells in an Animal Model of Glaucoma. *Sci. Rep.* 6, 27532. doi:10.1038/srep27532
- Madeira, M. H., Rashid, K., Ambrósio, A. F., Santiago, A. R., and Langmann, T. (2018). Blockade of Microglial Adenosine A2A Receptor Impacts Inflammatory Mechanisms, Reduces ARPE-19 Cell Dysfunction and Prevents Photoreceptor Loss *In Vitro*. *Sci. Rep.* 8, 2272. doi:10.1038/s41598-018-20733-2
- McIntosh, H. H., and Blazynski, C. (1994). Characterization and Localization of Adenosine A2 Receptors in Bovine Rod Outer Segments. *J. Neurochem.* 62, 992–997. doi:10.1046/j.1471-4159.1994.62030992.x
- Nobre, H. V., Cunha, G. M., de Vasconcelos, L. M., Magalhães, H. I., Oliveira Neto, R. N., Maia, F. D., et al. (2010). Caffeine and CSC, Adenosine A2a Antagonists, Offer Neuroprotection against 6-OHDA-Induced Neurotoxicity in Rat Mesencephalic Cells. *Neurochem. Int.* 56, 51–58. doi:10.1016/j.neuint.2009.09.001
- Ongini, E. (1998). SCH58261: A Selective A2A Adenosine Receptor Antagonist. *Drug Dev. Res.* 42, 63–70.
- Ostwald, P., Park, S. S., Toledano, A. Y., and Roth, S. (1997). Adenosine Receptor Blockade and Nitric Oxide Synthase Inhibition in the Retina: Impact upon post-ischemic Hyperemia and the Electroretinogram. *Vis. Res.* 37, 3453–3461. doi:10.1016/S0042-6989(96)00222-2
- Paterniti, I., Melani, A., Cipriani, S., Corti, F., Mello, T., Mazzon, E., et al. (2011). Selective Adenosine A2a Receptor Agonists and Antagonists Protect against Spinal Cord Injury through Peripheral and central Effects. *J. Neuroinflammation* 8, 31. doi:10.1186/1742-2094-8-31
- Perígolo-Vicente, R., Ritt, K., Gonçalves-de-Albuquerque, C. F., Castro-Faria-Neto, H. C., Paes-de-Carvalho, R., and Giestal-de-Araujo, E. (2014). IL-6, A1 and A2AR: a Crosstalk that Modulates BDNF and Induces Neuroprotection. *Biochem. Biophys. Res. Commun.* 449, 477–482. doi:10.1016/j.bbrc.2014.05.036
- Rey, H. L., and Burnside, B. (1999). Adenosine Stimulates Cone Photoreceptor Myoid Elongation via an Adenosine A2-like Receptor. *J. Neurochem.* 72, 2345–2355. doi:10.1046/j.1471-4159.1999.0722345.x
- Rosim, F. E., Persike, D. S., Nehlig, A., Amorim, R. P., de Oliveira, D. M., and Fernandes, M. J. (2011). Differential Neuroprotection by A(1) Receptor Activation and A(2A) Receptor Inhibition Following Pilocarpine-Induced Status Epilepticus. *Epilepsy Behav.* 22, 207–213. doi:10.1016/j.yebeh.2011.07.004
- Roth, S., Rosenbaum, P. S., Osinski, J., Park, S. S., Toledano, A. Y., Li, B., et al. (1997). Ischemia Induces Significant Changes in Purine Nucleoside Concentration in the Retina-Choroid in Rats. *Exp. Eye Res.* 65, 771–779. doi:10.1006/exer.1997.0391
- Santiago, A. R., Baptista, F. I., Santos, P. F., Cristóvão, G., Ambrósio, A. F., Cunha, R. A., et al. (2014). Role of Microglia Adenosine A2A Receptors in Retinal and Brain Neurodegenerative Diseases. *Mediators Inflamm.* 2014, 465694. doi:10.1155/2014/465694
- Severns, M. L., Johnson, M. A., and Bresnick, G. H. (1994). Methodologic Dependence of Electroretinogram Oscillatory Potential Amplitudes. *Doc Ophthalmol.* 86, 23–31. doi:10.1007/BF01224625
- Soliño, M., López, E. M., Rey-Funes, M., Loidl, C. F., Larrayoz, I. M., Martínez, A., et al. (2018). Adenosine A1 Receptor: A Neuroprotective Target in Light Induced Retinal Degeneration. *PLoS One* 13 (6), e0198838. doi:10.1371/journal.pone.0198838
- Stella, S. L., Bryson, E. J., and Thoreson, W. B. (2002). A2 Adenosine Receptors Inhibit Calcium Influx through L-type Calcium Channels in Rod Photoreceptors of the Salamander Retina. *J. Neurophysiol.* 87, 351–360. doi:10.1152/jn.00010.2001
- Stone, T. W., Ceruti, S., and Abbracchio, M. P. (2009). Adenosine Receptors and Neurological Disease: Neuroprotection and Neurodegeneration. *Handb. Exp. Pharmacol.* 193, 535–587. doi:10.1007/978-3-540-89615-9_17
- Tebano, M. T., Martire, A., Chioldi, V., Ferrante, A., and Popoli, P. (2010). Role of Adenosine A(2A) Receptors in Modulating Synaptic Functions and Brain Levels of BDNF: a Possible Key Mechanism in the Pathophysiology of Huntington's Disease. *ScientificWorldJournal* 10, 1768–1782. doi:10.1100/tsw.2010.164
- Yang, Z., Huang, P., Liu, X., Huang, S., Deng, L., Jin, Z., et al. (2015). Effect of Adenosine and Adenosine Receptor Antagonist on Müller Cell Potassium Channel in Rat Chronic Ocular Hypertension Models. *Sci. Rep.* 5, 11294. doi:10.1038/srep11294
- Zhang, G., Franklin, P. H., and Murray, T. F. (1994). Activation of Adenosine A1 Receptors Underlies Anticonvulsant Effect of CGS21680. *Eur. J. Pharmacol.* 255, 239–243. doi:10.1016/0014-2999(94)90104-x
- Zhang, S., Zhou, R., Li, B., Li, H., Wang, Y., Gu, X., et al. (2017). Caffeine Preferentially Protects against Oxygen-Induced Retinopathy. *FASEB J.* 31, 3334–3348. doi:10.1096/fj.201601285R

Conflict of Interest: The authors declare that the research was conducted in the absence of any commercial or financial relationships that could be construed as a potential conflict of interest.

Publisher's Note: All claims expressed in this article are solely those of the authors and do not necessarily represent those of their affiliated organizations or those of the publisher, the editors, and the reviewers. Any product that may be evaluated in this article, or claim that may be made by its manufacturer, is not guaranteed or endorsed by the publisher.

Copyright © 2022 Soliño, Larrayoz, López, Rey-Funes, Bareiro, Loidl, Girardi, Martínez and López-Costa. This is an open-access article distributed under the terms of the Creative Commons Attribution License (CC BY). The use, distribution or reproduction in other forums is permitted, provided the original author(s) and the copyright owner(s) are credited and that the original publication in this journal is cited, in accordance with accepted academic practice. No use, distribution or reproduction is permitted which does not comply with these terms.

GLOSSARY

A1R adenosine receptor type A1

A2AR adenosine receptor type A2A

Cat catalog

CI continuous illumination

CNS central nervous system

Co. Company

CTL control

DNaseI deoxyribonuclease

ECL Enhanced Chemiluminescence

ERG electroretinography

GCL ganglion cell layer

GE General Electric

GFAP glial fibrillary acidic protein

h hour

HRP horseradish peroxidase

IHC immunohistochemistry

HP Hewlett Packard

Hz Hertz

IL illuminated

IL-1 β interleukin-1 β

IL-6 interleukin-6

INL inner nuclear layer

iNOS inducible nitric oxide synthase

IPL inner plexiform layer

IR immunoreactive

LIRD light-induced retinal degeneration

μ micron

μ V microvolt

mRNA messenger ribonucleic acid

NFL nerve fiber layer

NIH National Institutes of Health

OD optical density

ONL outer nuclear layer

OP oscillatory potential

OPL outer plexiform layer

PCR polymerase chain reaction

PHL photoreceptor layer

qRT-PCR quantitative reverse transcription polymerase chain reaction

RNA Ribonucleic Acid

ROI region of interest

RPE retinal pigment epithelium

RT room temperature

TNF- α tumor necrosis factor- α

TUNEL terminal deoxynucleotidyltransferase dUTP nick end labeling

V Volt

W Watt

WB Western Blot

w/v weight/volume

18S 18 Svedberg